Highly Uniform VCSELs Grown by Multi-wafer Production MBE

Juan Li, Shannon M. Hill, Joseph A. Middlebrooks, Cheng-Yu Chen, Wei Li, Jenn-Ming Kuo,
Kevin W. Vargason, Yung-Chung Kao and Paul R. Pinsukanjana

Intelligent Epitaxy Technology, Inc., 1250 E. Collins Blvd., Richardson, TX 75081
Email: pinsu@intelliepi.com; Phone: 972-234-0068 #102

Keywords: VCSELs, uniformity, MBE

Abstract

To address the rapidly growing Vertical-cavity surface-emitting lasers (VCSELs) market, we have developed a production Molecular Beam Epitaxy (MBE) platform capable of producing high quality VCSEL epi wafers. Epitaxy growth by MBE offers the advantage of more abrupt interfaces compared to other epitaxy growth techniques. This is particularly attractive for the growth of higher performance VCSEL device structures, which often require more precise control of the interfaces to achieve higher performance. Example includes high speed 850 nm VCSEL for data comm and 940 nm VCSEL for high power applications. A multi-wafer production MBE optimized for VCSEL growth was successfully developed based on a Riber 6000 platform. Less than 0.4% uniformity across the platen was achieved by optimizing MBE reactor configuration and growth condition.

INTRODUCTION

The demand for Vertical-cavity surface-emitting laser (VCSEL)-based technologies is expected to surge over the next several years due to increasing technology adoption for both existing and emerging applications. Several key application areas include optical communication, proximity sensing, infrared illumination, gesture recognition, and LIDAR [1-3]. In order for large scale VCSEL technology implementation to be viable, the manufacturing process has to become high yielding in key critical areas, which include epitaxy, processing, dicing, mounting and testing [4].

In this paper, we shall address the viability of using multi-wafer production MBE platform for VCSEL epi wafer manufacturing. Currently, Metal Organic Chemical Vapor Deposition (MOCVD) is the main technology platform for VCSEL epi wafer production. A comparison between using MBE and MOCVD for production VCSEL epi wafer is summarized in Table 1. While MOCVD is generally a faster epi growth technique, MBE offers more abrupt interfaces with more precise control of doping concentration. However, in order to achieve certain VCSEL performance target, slower MOCVD growth rates are used [5], thus reducing the significance of higher throughput advantage. In addition, MBE also offers the ability to reach higher doping concentration level. This is particularly attractive for device designs with tunnel junctions which use highly doped p-n junction.

TABLE I

COMPARISON BETWEEN MOCVD & MBE FOR PRODUCTION VCSEL EPI WAFER GROWTH

	MOCVD	**MBE**
Wafers per run	Up to 8×6"	Up to 7×6" (This work uses 4×6".)
Growth rate	• 1.5-3 µm/hr • Have to slow down for key layers [5]	• 1-2 µm/hr
Defect density	OK for <20 cm^{-2}	OK for <20 cm^{-2}
Material uniformity across wafer	• Uniformity degrades with more coating of chamber • Need cleaning every few weeks	• < 0.4% across platen • Stable throughout 6-12 months campaign
Growth temperature	500-700 °C	400-600 °C
Interface abruptness	Not as good unless the growth rate is reduced significantly	Atomic level
p-doping	More difficult to reach very high p-type doping range	Can reach 1e20 cm^{-3} p-type doping
n-doping	More difficult to dope GaAs	Can easily reach mid e18 cm^{-3}
Materials purity	Hydrogen incorporation from metal organic source and carrier gas	No hydrogen
Maintenance duration	Few days plus re-calibration	4-6 weeks; no need to clean throughout the campaign
Maintenance frequency	Once every few weeks at full capacity	Once every 6-12 months
Safety handing	Require safety handling for hydrogen and hydride sources	High purity metals sources

The challenges associated with production epi wafer growth are typically driven by the balancing act to achieve sufficient performance and yield while maintaining an effective cost structure. Since requirements for VCSEL epi wafer growth are quite stringent, epitaxy growth stability and uniformity is more critical than for other optoelectronic devices [6]. Some of the key yield issues for VCSEL epi wafer growth are related to the control of the distributed Bragg reflectors (DBR) reflectivity stop-band (SB) center wavelength, the Fabry-Perot (F-P) dip wavelength and quantum well (QW) photoluminescence (PL) wavelength. Typically, the accuracy level has to be within a few nanometers. This requires the optical thickness to be controlled with its variation to well below 1% with ~0.5 % level being quite typical. Fluctuation or drift in the growth rate and/or growth condition across each wafer and from wafer to wafer during the growth run, or from run to run can shift the wavelengths of the F-P dip and SB center [7].

Precise control of F-P dip and SB center wavelengths is achieved by utilizing *in-situ* white light (WL) reflectivity monitoring for real-time growth condition adjustments. Excellent optical reflectivity uniformity of less than 0.4% across the 3", 4" and 6" platens with Riber 6000 multi-wafer production MBE platform has been demonstrated.

EXPERIMENTS

The results presented in this paper were based on typical p-on-n top illuminating GaAs-based VCSEL structure designs. The active region/resonant cavity with QWs are sandwiched between n-type and p-type DBRs. These designs also include high aluminum composition layer used for creating oxide dielectric aperture. These VCSEL epi wafers were grown using Riber 6000 reactors which are capable of supporting various platen configurations such as 15×3", 7×4", 9x4" or 4×6" as shown in Figure 1. The production MBE reactor setups for VCSEL growth were especially optimized to improve epitaxy layer thickness uniformity and growth stability necessary to address the stringent optical cavity requirements. AlGaAs compositional grades for various layers such as compositional grade up and down for DBR growths are achieved by utilizing a digital alloy combination approach by using multiple Al and Ga effusion cells, which are set to different growth rates. This digital alloy combination approach takes advantage of the stability of the large capacity Group III effusion cells on production MBE to achieve stable growth condition throughout each VCSEL growth run. Si effusion cell is used for n-type doping. Multi-orifice gas source CBr_4 system is utilized for p-type doping control. The current CBr_4 system used is set up with back pressure control in combination with 6 orifices ranging in various hole sizes to span various leak rates which enable a wide-dynamic range (from 10^{16} cm^{-3} to low-10^{20} cm^{-3}). This approach makes it possible to achieve both wide dynamic range and fast response for carbon doping control to accommodate more complex doping design profiles as required in more advanced VCSEL designs. Figure 2 shows an example of CBr_4 doping concentration obtained by Hall measurement vs. orifice area at a fixed growth rate and CBr_4 flow pressure setting.

These production MBE reactors are equipped with a suite of *in-situ* sensor capabilities for real-time process monitoring. The *in-situ* sensor capabilities include the following [8]:

- Absorption band-edge spectroscopy (ABES) and optical pyrometry for substrate temperature monitoring.
- Reflection high-energy electron diffraction (RHEED) for surface reconstruction and growth rate.
- White light (WL) optical reflectivity for monitoring DBR reflectivity spectra.
- Atomic Absorption Optical-based Flux Monitor (OFM) for Group III fluxes.

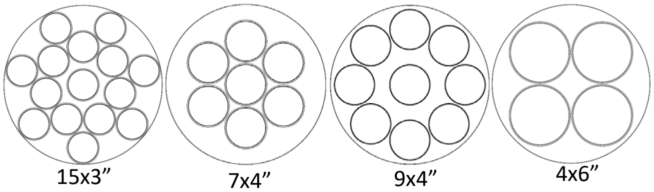

Fig. 1 Platen configurations available for Riber 6000: 15×3", 7×4", 9×4"and 4×6".

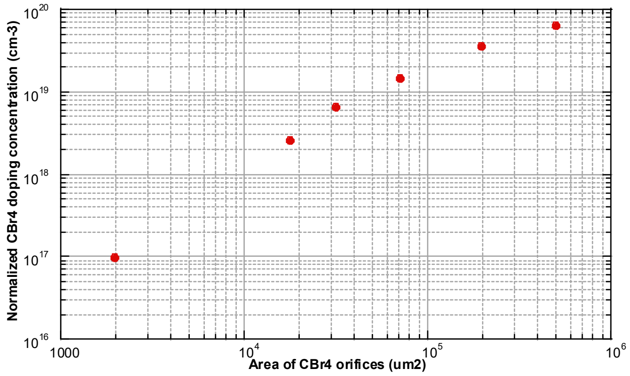

Fig. 2 Normalized CBr4 doping concentration obtained by Hall measurement as a function of the area of the CBr_4 orifices.

RESULTS AND DISCUSSION

Prior to the VCSEL structure growth, QW test structures were grown to optimize the optical characteristics by varying the substrate temperature, V/III ratio and other growth conditions. Bio-Rad/Nanometrics RPM 2000 tools were used for PL measurements. The PL peak uniformity across the wafer is mainly determined by the uniformity of the thickness and composition of the QWs. Figure 3 shows the typical PL peak wavelength maps and radial line scans across the 4" GaAs wafers loaded in the center and side slots of the 7×4" platens. The PL peak wavelengths of the

InGaAs QWs test structure from the center and side wafers vary from 880.2 nm to 881.3 nm which corresponds to ~ 1 nm variation within the growth run — less than 0.2% in PL wavelength uniformity.

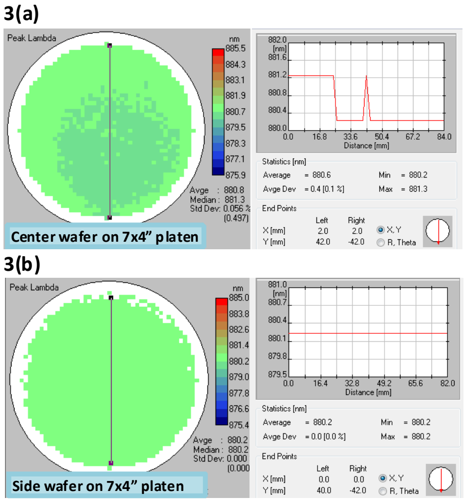

3(a)

Avge : 880.8
Median : 881.3
Std Dev: 0.056 %
(0.497)

Statistics [nm]
Average = 880.6 Min = 880.2
Avge Dev = 0.4 [0.1 %] Max = 881.3

End Points

	Left	Right
X [mm]	2.0	2.0
Y [mm]	42.0	-42.0

● X, Y
○ R, Theta

3(b)

Avge : 880.2
Median : 880.2
Std Dev: 0.000
(0.000

Statistics [nm]
Average = 880.2 Min = 880.2
Avge Dev = 0.0 [0.0 %] Max = 880.2

End Points

	Left	Right
X [mm]	0.0	0.0
Y [mm]	40.0	-42.0

● X, Y
○ R, Theta

Fig. 3 PL peak wavelength maps and radial line scans grown on the (a) center (b) side 4” GaAs substrates in a Riber 6000 MBE reactor (7×4”).

To reduce the run-to-run variations, *in-situ* WL monitoring is very critical for such complex VCSEL structures with a very long growth time. Figure 4 shows *in-situ* WL reflectivity spectra taken at the completion of various DBR periods during the bottom n-DBR growth. The spectra are captured automatically at the critical steps programmed into the growth recipe. Based on the established correlation between *in-situ* WL reflectivity data with the post-growth reflectivity data measured by Nanometrics RPM 2000 tool, real-time growth rate or growth time adjustments are made to ensure that the target optical cavity specifications can be reached.

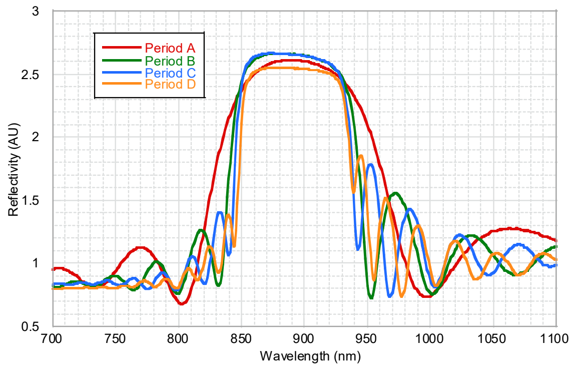

Fig. 4 In-situ WL reflectivity spectra recorded at different DBR periods during MBE growth of a VCSEL structure.

The full VCSEL growths were done in the production Riber 6000 MBE system on 15×3”, 7×4”, 9×4” and 4×6” platens using 850 nm or 940 nm VCSEL structures. Take the 850 nm VCSEL growths on the 7×4” platen as an example: the typical reflectivity maps and radial line scans of F-P Dip across the 4” center and side wafers are shown in Figure 5. The F-P dip wavelengths from the center wafer to the side wafer vary from 849.2 nm to 850.7 nm, which is well below 2 nm in variation or below 0.2%. The typical reflectivity maps and radial line scans of SB center across the 4” center and side wafers are shown in Figure 6. SB center wavelengths from the center wafer to the side wafer vary from 848.9 nm to 850 nm, which is well below 2 nm in variation or below 0.2%. The F-P dip and SB center wavelengths of all 7 wafers are well within the spec of 850 ± 2 nm. From the optical thickness points of view, the yield of all 7 of the 4” 850 nm VCSEL wafers is 100%.

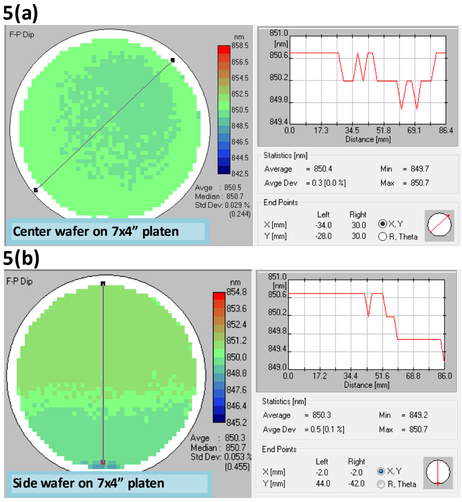

5(a)

Avge : 850.5
Median : 850.7
Std Dev: 0.029 %
(0.244)

Statistics [nm]
Average = 850.4 Min = 849.7
Avge Dev = 0.3 [0.0 %] Max = 850.7

End Points

	Left	Right
X [mm]	-34.0	30.0
Y [mm]	-28.0	30.0

● X, Y
○ R, Theta

5(b)

Avge : 850.3
Median : 850.7
Std Dev: 0.053 %
(0.455)

Statistics [nm]
Average = 850.3 Min = 849.2
Avge Dev = 0.5 [0.1 %] Max = 850.7

End Points

	Left	Right
X [mm]	-2.0	-2.0
Y [mm]	44.0	-42.0

● X, Y
○ R, Theta

Fig. 5 Reflectivity maps and radial line scans of F-P Dip across 850-VCSEL grown on the (a) center (b) side 4” GaAs substrate in a Riber 6000 MBE reactor (7×4”).

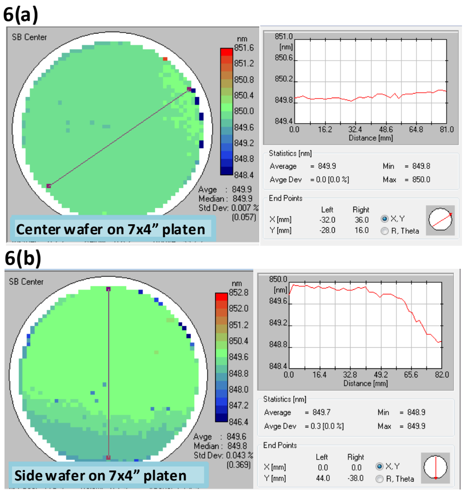

6(a)

Avge : 849.9
Median : 849.9
Std Dev: 0.007 %
(0.057)

Statistics [nm]
Average = 849.9 Min = 849.8
Avge Dev = 0.0 [0.0 %] Max = 850.0

End Points

	Left	Right
X [mm]	-32.0	36.0
Y [mm]	-28.0	16.0

● X, Y
○ R, Theta

6(b)

Avge : 849.6
Median : 849.8
Std Dev: 0.043 %
(0.369)

Statistics [nm]
Average = 849.7 Min = 848.9
Avge Dev = 0.3 [0.0 %] Max = 849.9

End Points

	Left	Right
X [mm]	0.0	0.0
Y [mm]	44.0	-38.0

● X, Y
○ R, Theta

Fig. 6 Reflectivity maps and radial line scans of SB center across 850-VCSEL grown on the (a) center (b) side 4” GaAs substrate in a Riber 6000 MBE reactor (7×4”).

The typical reflectivity maps and radial line scans of both F-P Dip and SB center across the 6” in diameter 940 nm VCSEL wafer on the 4x6” platen are also measured. The wavelength variations of F-P Dip and SB center are <1 nm and <2 nm across the 6” wafer respectively. Excellent uniformity of less than 0.3 % is achieved across the 6” VCSEL wafer.

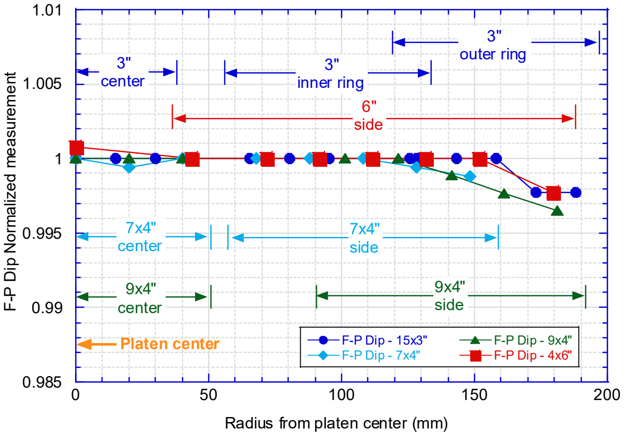

Fig. 7 Normalized F-P dip wavelength vs. radial distance from platen center for the 15x3”, 7x4”, 9x4” and 4x6” platens in a Riber 6000 MBE reactor.

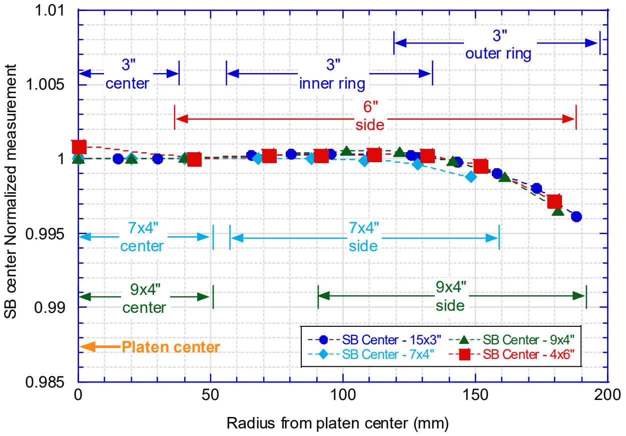

Fig. 8 Normalized SB center wavelength vs. radial distance from platen center for the 15x3”, 7x4”, 9x4” and 4x6” platens in a Riber 6000 MBE reactor.

Normalized uniformity profiles of F-P Dip for 15×3”, 7×4”, 9×4” and 4×6” platens are plotted in Figure 7. The measured F-P dip is normalized to the wavelength of a witness piece at the center of the platen. Wavelength uniformity of less than 0.4% for F-P dip is achieved for all VCSEL wafers grown on the different sizes of platens. The plot also shows that for up to 150 mm radius from the platen center, F-P dip is maintained at the same wavelength or only 0.1% drop. Most of the uniformity drop (less than 0.3%) occurs towards at the outer edge of the platen from radius of 150 mm to 200 mm. Of all the platens, 7×4” platen exhibits the best uniformity with only about 0.1% across the whole wafer surface areas on the platen. Normalized uniformity profiles of SB center for 15×3”, 7×4”, 9×4” and 4×6” platens are also plotted in Figure 8. The uniformity data of SB center is consistent with that of the F-P Dip.

The as-grown surface mapping of VCSEL wafers were performed using 0.8-7.7 µm diameter scan range with a KLA Tencor 6220 Surface scan tool with particle density of < 20 /cm^2.

CONCLUSIONS

Epitaxial growth of VCSEL for volume production is particularly challenging due to the stringent requirements in terms of uniformity across epi-wafer and the precise control necessary to match the various optical targeting requirements. In this work, a multi-wafer production MBE especially configured to support production VCSEL growth has been demonstrated.

ACKNOWLEDGEMENTS

The authors would like to thank the VCSEL production and characterization staff at IntelliEPI for their support.

REFERENCES

[1] O. M. Khreis, Computational Condensed Matter **9**, (2016).
[2] C. Yu-Chia, et al., Appl. Phys. A Mater. Sci. Process. **95,** 1033 (2009).
[3] C. J. Chang-Hasnain, et al., Appl. Phys. Lett. **58**, 31 (1991).
[4] R. Jäger, *Mass production of optoelectronic devices*, Molecular Beam Epitaxy, pp. 681-695, 2013.
[5] J. A. Tatum, Vertical Cavity Surface Emitting Lasers in Data Networks and Consumers Devices, 2016 CS MANTECH 2016 presentation, Miami, FL.
[6] C. Wilmsen, *Epitaxy of Vertical-Cavity Lasers*, Vertical-Cavity Surface-Emitting Lasers, pp. 158-160, 1999.
[7] R. Jäger, et al., Journal of Crystal Growth, **323**, 434 (2011).
[8] A. W. Jackson, P. R. Pinsukanjana, A. C. Gossard, and L. A. Coldren, In Situ Monitoring and Control for MBE Growth of Optoelectronic Devices, IEEE J. Selected Topics in Quantum Electronics, 3(3), 836 (1997).

ACRONYMS

VCSEL: Vertical-cavity surface-emitting lasers
MBE: Molecular Beam Epitaxy
LIDAR: LIght Detection And Ranging
DBR: Distributed Bragg reflectors
SB: Stop-band
F-P: Fabry-Perot
QW: Quantum well
PL: Photoluminescence
MOCVD: Metal Organic Chemical Vapor Deposition
WL: White light
RHEED: Reflection high-energy electron diffraction
ABES: Absorption band-edge spectroscopy